Enhancement of Surface Graft Density of MPEG on Alginate/Chitosan Hydrogel Microcapsules for Protein Repellency

ARTICLE *in* LANGMUIR · AUGUST 2012

Impact Factor: 4.46 · DOI: 10.1021/la302615t · Source: PubMed

13 AUTHORS, INCLUDING:

Hongguo Xie
Dalian Institute of Chemical Physics
28 PUBLICATIONS **240** CITATIONS
SEE PROFILE

Mingqian Tan
Dalian Polytechnic University
69 PUBLICATIONS **1,156** CITATIONS
SEE PROFILE

Gong faquan Faquan
Chinese Academy of Sciences
5 PUBLICATIONS **31** CITATIONS
SEE PROFILE

Xiudong Liu
Dalian Institute of Chemical Physics
46 PUBLICATIONS **1,050** CITATIONS
SEE PROFILE

Langmuir

Article

pubs.acs.org/Langmuir

Enhancement of Surface Graft Density of MPEG on Alginate/Chitosan Hydrogel Microcapsules for Protein Repellency

Jiani Zheng,[†,⊥] Hongguo Xie,*[,†] Weiting Yu,[†] Mingqian Tan,[†] Faquan Gong,[§] Xiudong Liu,*[,‡] Feng Wang,[∥] Guojun Lv,[†] Wanfa Liu,[§] Guoshuang Zheng,[†,⊥] Yan Yang,[†,⊥] Weiyang Xie,[†] and Xiaojun Ma[†]

[†]Laboratory of Biomedical Material Engineering, [§]Laboratory of Coil Efficiency and Optical Resonator, and [∥]Laboratory of Optical Fabrication and Coating, Dalian Institute of Chemical Physics, Chinese Academy of Sciences, Dalian 116023, China

[‡]College of Environment and Chemical Engineering, Dalian University, Dalian Economic Technological Development Zone, Dalian 116622, China

[⊥]Graduate School of the Chinese Academy of Sciences, Beijing 100049, China

Supporting Information

ABSTRACT: Alginate/chitosan/alginate (ACA) hydrogel microcapsules were modified with methoxy poly(ethylene glycol) (MPEG) to improve protein repellency and biocompatibility. Increased MPEG surface graft density (n_S) on hydrogel microcapsules was achieved by controlling the grafting parameters including the buffer layer substrate, membrane thickness, and grafting method. X-ray photoelectron spectroscopy (XPS) model was employed to quantitatively analyze n_S on this three-dimensional (3D) hydrogel network structure. Our results indicated that neutralizing with alginate, increasing membrane thickness, and in situ covalent grafting could increase n_S effectively. $ACAC_{PEG}$ was more promising than ACC_{PEG} in protein repellency because alginate supplied more $-COO^-$ negative binding sites and prevented MPEG from diffusing. The n_S increased with membrane thickness, showing better protein repellency. Moreover, the in situ covalent grafting provided an effective way to enhance n_S, and 1.00 ± 0.03 chains/nm^2 was achieved, exhibiting almost complete immunity to protein adsorption. This antifouling hydrogel biomaterial is expected to be useful in transplantation in vivo.

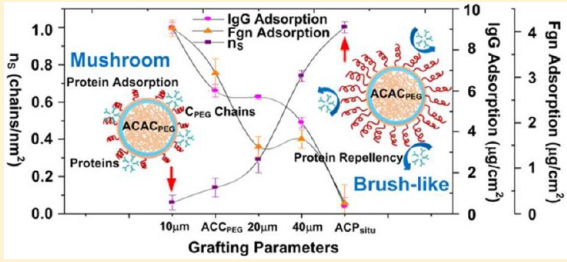

1. INTRODUCTION

Encapsulating live cells and tissues within a protective hydrogel membrane is proposed as a promising method to preclude the problems associated with immune rejection during allogenic and xenogenic transplantation.[1−4] The polymeric hydrogel semipermeable membrane with a three-dimensional (3D) network structure[5,6] not only remains permeable to the low molecular weight species, such as nutrients, metabolites, and transport proteins, for cell proliferation and function,[7] but also provides immunoprotection, which restricts the ingress of antibodies and complement fractions to prevent any direct contact between the entrapped cells and their surrounding environment.

Alginate/chitosan/alginate (ACA) hydrogel microcapsules are commonly used for the immunoprotection of transplanted therapeutic cells due to their nonimmunogenic and nontoxic properties.[8−11] However, the fibrous overgrowth of the microcapsules remains a concern. The development of fibrotic tissue around the implanted microcapsules hinders the diffusion of cell nutrients and therapeutic products across the capsule membrane, resulting in transplant failure and hampering the progress of encapsulated cell transplantation.[12] Protein adsorption[13] on the surface of the microcapsules is generally considered a criminal that causes an inflammatory response and consequent fibrous overgrowth. Surface modification of microcapsules is of great importance in eliminating the nonspecific adsorption of proteins in the design of transplantation devices.

Poly(ethylene glycol) (PEG) has the extraordinary ability of protein resistance, which is attributed to a number of unique properties such as minimum interfacial free energies with water, extensive hydration, good conformational flexibility, considerable chain mobility, and large excluded volume.[14] Moreover, PEG's low toxicity and low immunogenicity on the FDA's safe list make it a suitable material for applications in the field of transplantation devices.[15]

Recent studies of PEG modification have focused on the self-assembly monolayer (SAM) on metal or crystalline substrates, which demonstrates the important role of PEG surface coverage in protein resistance.[16−23] The results implied that the conformation of surface-grafted PEG varies from mushroom (random coil) to brush forms (helical) with overlapping regimes.[24] At lower graft density, the interaction between the

Received: June 29, 2012
Revised: August 21, 2012
Published: August 24, 2012

neighboring PEG chains is negligible, as in the case where PEG chains distribute discretely, exhibiting a mushroom conformation with no protein repellency. As the graft density increases, the overlapped PEG chains stretch away from the surface to form a brush-like conformation, which strengthens protein repellency.[25] We have studied methoxy poly(ethylene glycol) (MPEG) modified ACA hydrogel microcapsules.[26] It has been found that MPEG chains can not only bind onto the surface, but also interpenetrate a certain depth into the membrane of ACA microcapsules with 3D hydrogel network structure, which is quite complex compared to the situation in the monolayer system. Moreover, the interpenetrated portion has little effect on protein repellency, because the brush-like chains cannot stretch out to the surface to repel protein.[26] Therefore, it is especially crucial to quantitatively determine the relationship between the MPEG chains bound to microcapsule surface, that is, MPEG surface graft density (n_S, chains/nm^2), and protein repellency, which is helpful to determine strategy of guiding more MPEG chains to gather on the surface for protein repellency.

In this paper, to increase MPEG surface coverage on hydrogel microcapsules, different grafting parameters of MPEG such as the buffer layer substrate, membrane thickness, and grafting method were investigated. The strategies included adding an alginate buffer layer to neutralize surface charge, supply more carboxyl ($-COO^-$) negative binding sites and hinder the diffusion of MPEG chains, and reducing steric hindrance by in situ covalent grafting to enhance n_S, and then get high resistance to gamma globulin (IgG) and fibrinogen (Fgn) protein adsorption. Due to the close relationship between n_S and protein repellency, a quantitative analysis method using X-ray photoelectron spectroscopy (XPS) was also developed to determine n_S on hydrogel microcapsules, and the corresponding protein repellency was investigated.

2. EXPERIMENTAL SECTION

2.1. Materials. MPEG of M_n 2000 g mol^{-1} was purchased from Sigma Aldrich Chemical Co. (USA). Chitosan with M_w of 20 kDa was degraded from raw material (Yuhuan Ocean Biomaterials Corporation, Zhejiang, China) in our laboratory, showing the polydispersity index (PDI) of 1.4 measured by gel permeation chromatography (GPC) technique.[27] The degree of deacetylation (DD) was about 95% as determined by ^{1}H NMR. The chitosan-grafted-MPEG2K-DS21% (CS-g-MPEG2K-DS21%) copolymer was synthesized and characterized as previously described.[26] The CS-g-MPEG2K-DS21% had a 20 kDa chitosan backbone and was grafted by 2 kDa MPEG side chains with a degree of substitution (DS) of 21%. The terminal hydroxyl of MPEG was modified by bromoacetaldehyde diethylacetal (BADA, Sigma, USA) according to the Williamson nucleophilic substitution reaction,[28] in which the product was abbreviated as MPEG-BADA. Sodium alginate (Qingdao Crystal Salt Bioscience and Technology Corporation, Qingdao, China) with a viscosity of 230 cP at a concentration of 1% w/v in 0.9% w/v NaCl aqueous solution at 25 °C was purchased. Fluoresceinamine (Sigma, USA) labeled alginate was prepared according to the method developed by Strand et al.[29] Rhodamine-B (Sigma, USA) labeled chitosan was prepared according to the method developed by our laboratory.[30] Fluorescein isothiocyanate (FITC, isomer I, Sigma, USA) labeled CS-g-MPEG was synthesized according to the method by Hiraku et al.[31] Sodium cyanoborohydride ($NaCNBH_3$) was obtained from Fluka Chemical Co. (USA). Gamma globulin (IgG, Bovine Blood) and fibrinogen (Fgn, Bovine Blood) were purchased from Sigma Aldrich Chemical Co. (USA) and used without any pretreatment. All the other reagents or chemicals were all analytical-grade and used without further purification.

2.2. Preparation of MPEG-Modified Hydrogel Microcapsules. Strategies of PEG surface modification include the layer-by-layer (LBL) polyelectrolyte self-assembly of PEG-grafted copolymers and the covalent surface immobilization via "grafting to" method.[14,32−34] Regarding the LBL polyelectrolyte self-assembly method, PEG was grafted as the side chains onto a cationic polyelectrolyte backbone such as poly(L-lysine)[35,36] and chitosan.[16,20] As for covalent grafting method, the functionalized PEG molecules with appropriate terminal groups were grafted onto substrates via suitable chemical reactions.[37]

2.2.1. LBL Polyelectrolyte Self-Assembly Method. The method details can be found in our previous work.[26] In brief, calcium alginate gels were generated as the core of microcapsules, and then chitosan diffused into and bound on the gels to form AC membranes. Another alginate layer was formed as a buffer layer to neutralize positive charge and supply $-COO^-$ negative binding sites for further CS-g-MPEG layer (C_{PEG}) grafting. The ACC_{PEG} microcapsules without alginate buffer layer were prepared with the same procedure as the control. The ACAC microcapsules were also prepared as control to test protein repellency.

To further study the influence of alginate buffer layer substrate on n_S and protein repellency, $ACAC_{PEG}$ microcapsules with different membrane thicknesses (10, 20, 40 μm) of ACA were prepared with different coating time (5, 20, 50 min), respectively.

2.2.2. In Situ Covalent Grafting Method. ACP_{situ} microcapsules were fabricated by in situ covalent grafting method, in which the covalently grafted MPEG layer was abbreviated as P_{situ}. In detail, the fabricated AC microcapsules were incubated in the terminal aldehyde MPEG (MPEG-CHO) solution that was attained from in situ hydrolysis of MPEG-BADA[38] for one hour while adding $NaCNBH_3$ aqueous solution dropwise at room temperature under nitrogen protection to get ACP_{situ} microcapsules.

2.3. Preparation of MPEG-Modified Hydrogel Membranes. The microcapsules mentioned above were used for protein repellency testing, and the corresponding flat membranes simulating microcapsule membranes were prepared for XPS[39,40] and surface roughness characterization. Alginate solution (1.5% w/v) was cast onto a dry glass slide, which was then immersed in a 1.1% w/v $CaCl_2$ solution to form calcium alginate gels. After gelling for 30 min, the slides with gel were incubated in 0.5% w/v chitosan solution for different coating times to form AC membranes with different thicknesses. The slides with AC membranes were subsequently rinsed with 0.9% w/v NaCl solution. A 0.15% w/v alginate solution was added to counteract excessive charges on the membrane. The ACA membranes were then washed thoroughly with 0.9% w/v NaCl solution. Then, the slides with $ACAC_{PEG}$ membranes were obtained by incubation of ACA membranes in 1.0% w/v CS-g-MPEG2K-DS21% solution for 45 min. The control ACC_{PEG} membranes without alginate incubation and the AC and ACA membranes were all fabricated with the same method as $ACAC_{PEG}$ membranes. The ACP_{situ} membranes were prepared by incubating AC membranes into the mixed solution of MPEG-CHO hydrolyzed from MPEG-BADA and $NaCNBH_3$ for one hour at room temperature under nitrogen protection. At last, all the membranes were washed thoroughly with Milli-Q water. The powdered sample of CS-g-MPEG2K-DS21% was pressed into a small square disk for XPS analysis. For XPS measurement, all samples were fully dehydrated by allowing them to slowly air-dry for a minimum of 24 h before keeping them in a vacuum desiccator for at least 24 h.

2.4. XPS Measurements. XPS spectra were used to characterize the surface information by an Escalab 250 Xi X-ray photoelectron spectrometer (Thermo Scientific). The X-ray originated from an unmonochromated Al Kα anode was operated at 1486.6 eV and powered at 300 W. The signal was gathered from a sample area of 0.5 × 0.5 mm at a takeoff angle of 45° with respect to the sample plane, and the approximate depth of profile was 2−10 nm. High-resolution spectra of carbon (C_{1s}) and oxygen (O_{1s}) peaks were recorded at analyzer pass energy of 20 eV, which allowed additional surface sensitivity because atomic charge states can be resolved with more details and with a detection error of less than 1%.[41] Charge shift

corrections were made by setting C_{1s} peaks of saturated hydrocarbons (C−C) to 285.0 eV.[42] Spectral analysis was performed using the *XPS Peak* software v 4.1. High-resolution spectra were resolved into individual Gaussian−Lorentzian peaks using a least-squares fitting program and the Gaussian/Lorentzian ratio was set to 50%.

2.5. Measurement of MPEG Surface Graft Density. To quantitatively analyze the MPEG surface coverage, the surface graft density (n_S, chains/nm^2) was defined as the number of molecules per unit area on membrane surface within the depth of several nanometers, which was calculated by XPS analysis.

The thickness (d, nm) of MPEG layer could be calculated using the model established by Damodaran et al,[43] as the following eq 1:

$$d = \left(\frac{49}{E^2\rho} + 0.11\frac{\sqrt{E}}{\rho}\right)\sin\theta\left(\frac{A}{A_0} + 1\right) \quad (1)$$

where ρ is the density of CS-g-MPEG (0.98 g/cm^3), which can be deduced from literature[15] in the LBL polyelectrolyte self-assembly method, and in the in situ covalent grafting method, ρ is the density of MPEG (1.1 g/cm^3);[43] the electron energy E can be given as 1201 eV,[43] and θ is the electron takeoff angle (45°) of X-rays on the sample surface. A_0 and A are ether carbon (C−O−C) peak area percentages of C_{1s} spectra before and after MPEG grafting, according to the eq 2:

$$A \text{ or } A_0\,(\%) = \frac{A_{C-O-C}}{A_{C-O-C} + A_{O=C-O} + A_{O=C-NH} + A_{C-C}} \times 100\% \quad (2)$$

where A_{C-O-C}, $A_{O=C-O}$, $A_{O=C\text{-}NH}$ and A_{C-C} were peak area of C−O−C, O=C−O$^-$, O=C-NH and C−C peaks, respectively.

When MPEG layer thickness (d) was calculated using eq 1, a residual thickness d_{r1} of 5.50 nm and d_{r2} of 4.90 nm were observed as $A = A_0$ in the method of LBL polyelectrolyte self-assembly and in situ covalent grafting, respectively. This arbitrary residual thickness is characteristic of the particular instrument, material, and electron takeoff angle, and should be subtracted from the calculated values to obtain the absolute thickness (d_{abs}) as below:[43]

$$d_{abs} = d - d_r(\text{nm}) \quad (3)$$

In the LBL polyelectrolyte self-assembly method, the MPEG surface graft density (n_S, chains/nm^2) determined from ρ, d_{abs}, and DS could be calculated from the following eq 4:[17,44]

$$n_S = \frac{\rho d_{abs} N_A}{M_{chitosan}/DS + M_{PEG}} \quad (4)$$

where $M_{chitosan}$ and M_{PEG} are molecular weights of chitosan monomer and MPEG chain, respectively. N_A is Avogadro's number (6.023×10^{23} mol^{-1}), and DS is 21%. In the in situ covalent grafting method, the MPEG surface graft density (n_S, chains/nm^2) could also be calculated from the following eq 5:

$$n_S = \frac{\rho d_{abs} N_A}{M_{PEG}} \quad (5)$$

The reported data were the mean values of triplicate samples for each kind of membrane.

2.6. Measurement of Binding Amount of CS-g-MPEG. The binding amount (m_b, μg/cm^2) of CS-g-MPEG was defined as the mass of copolymers per unit area of microcapsules, which was determined by measuring the concentration decrease of CS-g-MPEG during the binding process with GPC technique established by Yu et al.[45] as the following eq 6:

$$m_b = \frac{(C_0 - C_n)V_t}{S} \quad (6)$$

where C_o and C_n are the initial CS-g-MPEG concentration and the CS-g-MPEG concentration in the supernatant after binding process, respectively; V_t is the total volume of the solution (1 mL); and S is the total sphere surface area of microcapsules. The reported data were the mean values of triplicate samples for each kind of microcapsule.

2.7. CLSM Measurements. Confocal laser scanning microscopy (CLSM) was employed to characterize the distribution of alginate, chitosan, and CS-g-MPEG in MPEG-modified microcapsules made by fluorescent-labeled polymers. The visual images and integral model were used for qualitative and quantitative analysis, respectively. The microcapsules were examined by a CLSM (Leica, TCS-SP2, Germany), equipped with Ar (488 nm/5 mW) and He−Ne (543 nm/1.2 mW) laser sources and an inverted microscope (Leica, DMIRE2, Germany). For image acquisition, the suspension of 0.05 mL fluorescent-labeled microcapsules in 0.3 mL NaCl solution (0.9% w/v) was placed in a chambered coverglass system (Lab-Tek). Two separate channels of CLSM were used in the green and red fluorescence modes at excitation wavelengths of 488 and 543 nm, respectively. The third channel was set to the transmitted light detector. All confocal fluorescence images were taken with a 20× objective (HC PLAN APO 20×/0.40 PH1 0.17/A 2.2). The focal planes were set at the equatorial sections of the microcapsules. For background and noise reduction, the images were generated by accumulating four scans per image. All images were acquired at constant microscopic settings under computer control in order to obtain comparable images.

For quantitative analysis of a uniform microcapsule, we randomly drew a diameter across the focal plane of the microcapsules and obtained its fluorescent intensity through computational profile analysis (Leica confocal software, Germany). The total fluorescent distribution information was represented and simplified by this horn-like intensity profile. The integral of fluorescent intensity curve along the diameter, which represented the total amount of polymer on the membrane, was calculated by eq 7:

$$I = \int_0^D f(x)\,dx \quad (7)$$

where I represents the integral of fluorescent intensity along the diameter across equatorial section; D is the diameter of hydrogel microcapsules; $f(x)$ is the function of the fluorescent intensity corresponding to the position on the diameter across equatorial section, which can be detected directly by CLSM. The integral of fluorescent intensity along twelve diameters randomly taken across equatorial sections of different microcapsules were averaged to obtain an average fluorescent intensity and standard deviation (SD).

2.8. Measurement of Protein Adsorption. Protein adsorption measurements were carried out based on the method described previously.[40] IgG and Fgn were used as model proteins to evaluate the protein-resistant characteristics of MPEG-modified microcapsules. Experiments were carried out in 10 mmol/L phosphate buffer (Na_2HPO_4/KH_2PO_4, pH 7.4) in order to keep a constant pH during the adsorption process. The microcapsules (0.1 mL) were incubated in protein solution (0.3 mL) with concentration of 1.0 mg/mL at 37 °C for 2 h[46] to imitate the protein adsorption process in vivo after biomaterials transplantation. The adsorbed amounts of protein were determined by measuring the difference of protein concentration before and after the adsorption process.[47] The amount (q) of the protein adsorbed on the microcapsules was calculated using the following eq 8:

$$q = \frac{(C_i - C_f)V}{S} \quad (8)$$

where C_i and C_f are the initial protein concentration and the protein concentration in the supernatant after adsorption studies, respectively; V is the total volume of solution (0.3 mL); and S is the total sphere surface area of microcapsules. The reported data were the mean values of triplicate samples for each kind of microcapsule.

2.9. Measurement of Zeta Potential. The zeta potential of microcapsules was measured using a Sur-PASS Electrokinetic analyzer (Anton Paar GmbH, Austria) equipped with a cylindrical cell. The streaming potential was measured by using Ag/AgCl electrodes. For each measurement, approximately 1.5 mL of wet microcapsules was transferred into the glass cylinder of the measuring cell. Before starting the measurement, the microcapsules were rinsed with double-distilled

dx.doi.org/10.1021/la302615t | *Langmuir* 2012, 28, 13261−13273

Scheme 1. Schematic Illustration of Grafting Process of MPEG on the Hydrogel Microcapsules (not to scale)

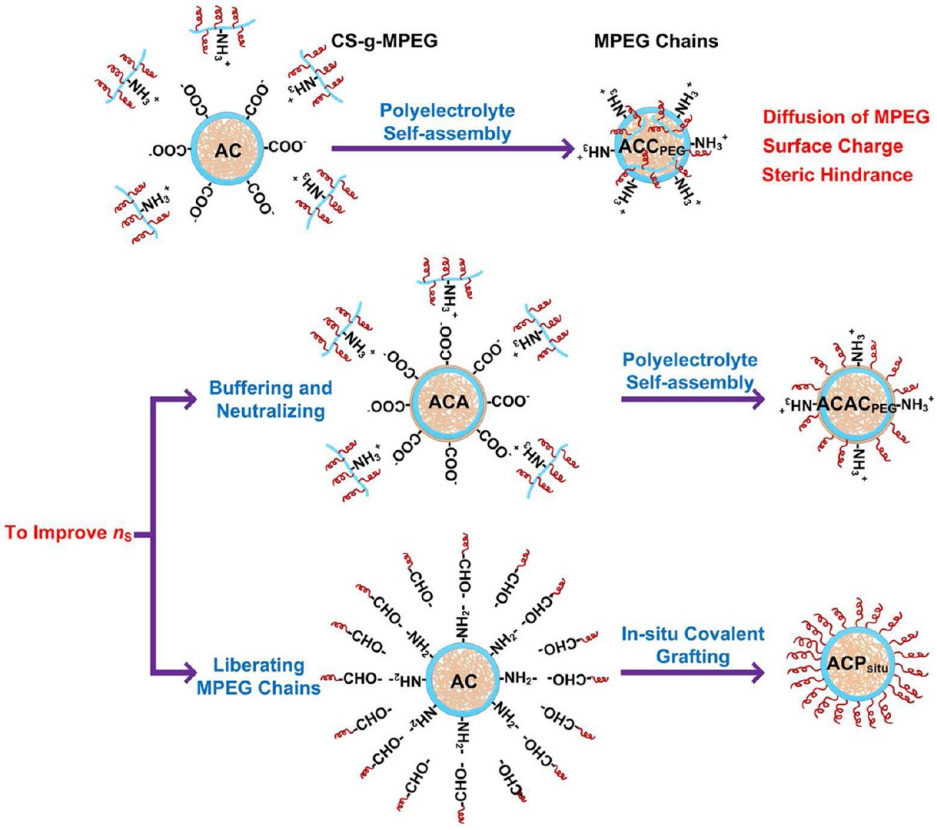

water to remove NaCl. A background electrolyte of 1 mmol/L KCl solution was used. The zeta potential (ξ, mV) was obtained from the streaming potential measurements based on the Smoluchowski equation[47−49] as follows:

$$\xi = \frac{dU_{str}}{dp}\frac{\eta K_B}{\varepsilon_0 \varepsilon_r} \quad (9)$$

where U_{str} is the streaming potential, p is the pressure drop across the streaming channel, ε_0 is the vacuum permittivity (8.854×10^{-12} $J^{-1}\cdot C^2\cdot m^{-1}$), ε_r is the dielectric constant of the aqueous solution (78.3), η is the electrolyte solution viscosity (0.8902 mPa·s), and K_B is the electrical conductivity of the bulk solution. Since the surface conductivity of the microcapsules cannot be determined directly, the zeta potential obtained from the streaming potential measurement using eq 9 is considered an apparent value.

2.10. Measurement of Surface Roughness. The surface roughness and surface morphology of hydrogel ACAC$_{PEG}$ microcapsule membrane with different membrane thickness in the wet state was measured by a noncontact, three-dimensional white-light optical interferometer (New-View 5020, ZYGO).[47] Before starting the measurement, free water on the surface of membranes was removed with absorbent paper from one side of the gel membrane. Average values were obtained from multiple roughness values (at least three) on different areas of each sample.

2.11. Statistical Analysis. Data were expressed as mean values ± SD of the replicate samples. Statistical comparisons were performed using a one-way analysis of variance (ANOVA). The p-values smaller than 0.05 were considered to indicate statistical significance.

3. RESULTS AND DISCUSSION

3.1. Strategies To Increase Surface Graft Density of MPEG Chains. The hydrogel microcapsules based on alginate and chitosan and the grafting process of MPEG on the microcapsules were shown in Scheme 1, which also elaborated the problems that might limit protein repellency. The problems included the diffusion of MPEG into porous hydrogel, surface positive charge on the microcapsules, and steric hindrance of brush-like CS-g-MPEG copolymer. First, the 3D network structure enabled the free diffusion of low-molecular-weight water-soluble molecules such as MPEG through porous hydrogels. The MPEG2K side chains had a helical structure with a length of ~12 nm[21] so that part of the MPEG chains distributed inside the 3D network could not stretch out to the surface and had little resistance to protein adsorption. Second, the positive sites on microcapsules were attributed to the protonated amino ($-NH_3^+$) groups of chitosan. The positive sites would do great harm to protein repellency, because most of proteins showed negative charges in physiological environment. Third, in CS-g-MPEG2K-DS21% copolymer, each chitosan backbone could only carry ~40 MPEG side chains, and the LBL self-assembly process of the brush-like CS-g-MPEG copolymer was limited by the steric hindrance effect of MPEG side chains, which significantly limited the n_S of MPEG chains. The low n_S would reduce protein repellency.

To solve the above three problems, it was important to increase MPEG chain density on the surface, neutralize positive sites, and liberate MPEG chains from chitosan backbone. As shown in Scheme 1, two strategies were developed to improve the protein repellency of microcapsules. First, a buffer layer was introduced to neutralize the positive charge on the surface, supply $-COO^-$ negative sites for CS-g-MPEG binding, and prevent MPEG chains from diffusing into microcapsules. Alginate, a natural polysaccharide used in the fabricating process of ACA microcapsules, was a polymer with negative charge and could be used as a buffer layer. For this purpose, in this study, the different grafting parameters including the buffer

dx.doi.org/10.1021/la302615t | Langmuir 2012, 28, 13261−13273

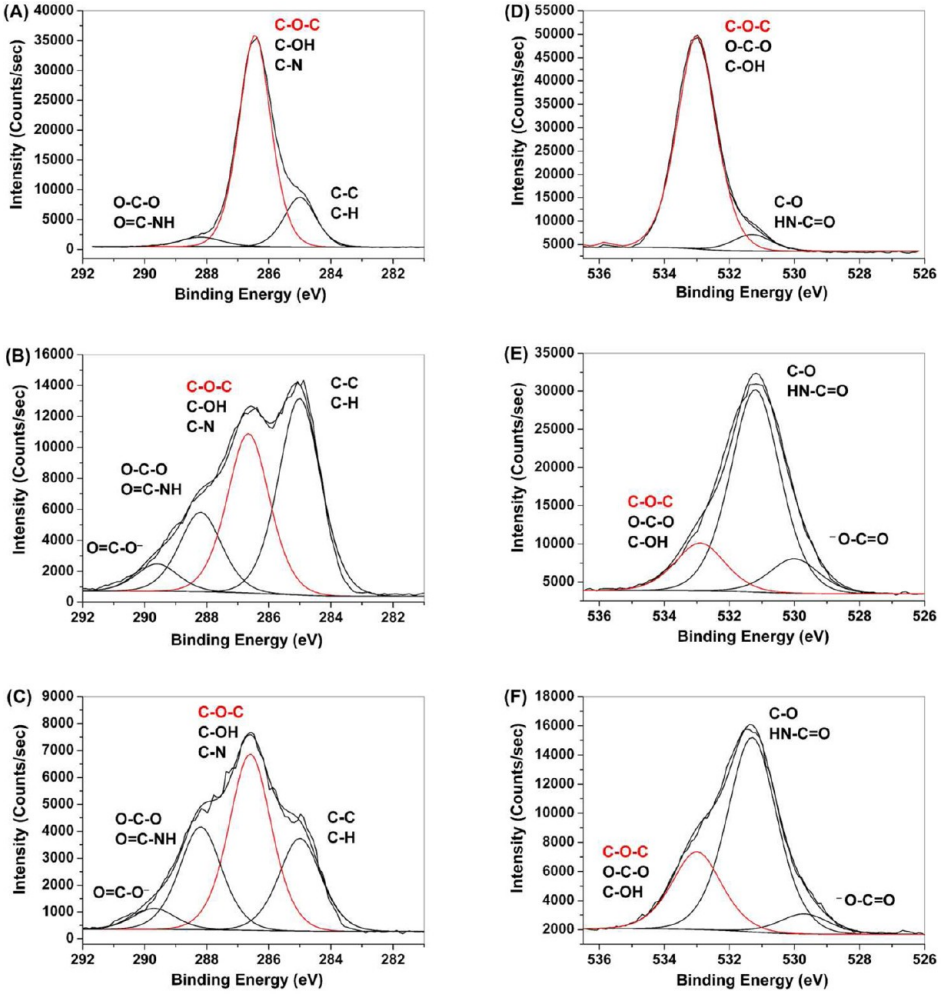

Figure 1. High-resolution XPS spectra for dehydrated CS-g-MPEG2K-DS21% copolymer, ACA and $ACAC_{PEG}$ microcapsule membranes, and their fitting curves. (A), (B), and (C) were C_{1s} peaks for CS-g-MPEG2K-DS21% copolymer, ACA, and $ACAC_{PEG}$, respectively. (D), (E), and (F) were O_{1s} peaks for corresponding samples.

Table 1. Peak Area Percentage (%) and Binding Energy (eV) for Carbon and Oxygen Species of the CS-g-MPEG2K-DS21% Copolymer, ACA, and $ACAC_{PEG}$ Microcapsule Membranes in a High Resolution Mode

	binding energy (eV) of C_{1s} (peak area percentage %)				binding energy (eV) of O_{1s} (peak area percentage %)		
	285	286.5	288	289	530	531	533
	C−C	C−O−C	HN−C=O	O=C−O^-	O=C−O^-	HN−C=O	C−O−C
CS-g-MPEG2K-DS21%	18.3	78.0	3.7	—	—	7.1	92.9
ACA	42.4	34.5	17.2	5.9	12.2	71.0	16.8
$ACAC_{PEG}$	23.6	44.9	26.1	5.3	6.8	66.6	26.6

layer substrate and membrane thickness were adjusted to concentrate more MPEG chains on the surface of microcapsules for protein repellency through an increasing amount of alginate buffer layer. Second, by the in situ covalent grafting method, the terminal modified-MPEG chains liberated from chitosan backbone were seeded directly onto the amino ($-NH_2$) groups of AC microcapsules without the steric hindrance. The terminal functional groups of MPEG could also occupy $-NH_2$ sites on AC microcapsules, which prevented $-NH_2$ from being protonized and shielded positive charge. Furthermore, to quantify MPEG surface graft density (n_S, chains/nm^2), XPS was employed to reveal the information of the outermost 2−10 nm of microcapsule membrane.

3.2. XPS Analysis. The C_{1s} and O_{1s} peaks can be peak-fitted to analyze the elements' binding states.[41,42,50−53] The percentage of a particular binding state varies in different materials, which can be used to deduce the existence of a particular material and qualitatively analyze the inherent law. Since each MPEG chain with molecular weight of 2000 g mol^{-1} has 44 repeat units of ether carbon (C−O−C), the introduction of MPEG on the surface of ACA membranes will strengthen the percentage of C−O−C binding state in C_{1s} and O_{1s} high-resolution XPS spectra.

High-resolution XPS spectra of CS-g-MPEG2K-DS21% copolymer, ACA, and $ACAC_{PEG}$ membranes and their fitting curves were shown in Figure 1, and the peak area percentages of different binding states were summarized in Table 1. The C_{1s}

dx.doi.org/10.1021/la302615t | Langmuir 2012, 28, 13261−13273

Table 2. Calculation of MPEG Surface Graft Density on MPEG-Modified Microcapsule Membranes with Different Grafting Parameters

grafting parameters		unmodified	modified	calculated data[a]		
		A_0 (%)	A (%)	d (nm)	d_{abs} (nm)	n_s (chains/nm^2)
alginate buffer layer	ACC_{PEG}	31.2	38.9 ± 2.4	6.2 ± 0.2	0.7 ± 0.2	0.14 ± 0.05
	$ACAC_{PEG}$	34.5	51.7 ± 4.1	6.9 ± 0.3	1.4 ± 0.3	0.29 ± 0.07
membrane thickness	10 μm	37.3	37.9 ± 7.0	5.5 ± 0.2	0.3 ± 0.2	0.06 ± 0.04
	20 μm	34.5	51.7 ± 4.1	6.9 ± 0.3	1.4 ± 0.3	0.29 ± 0.07
	40 μm	34.7	78.6 ± 1.9	9.0 ± 0.1	3.5 ± 0.1	0.74 ± 0.03
grafting method	ACP_{situ}	31.2	69.5 ± 1.0	7.9 ± 0.1	3.0 ± 0.1	1.00 ± 0.03

[a]Expressed as mean ± SD (n = 3).

peak of CS-g-MPEG2K-DS21% shown in Figure 1A could be resolved into three peaks representing aliphatic carbon (C−C),[42,51,52] C−O−C[41,42,50−52] of repeat units of MPEG chains and carbon−nitrogen (C−N) bonds in chitosan backbone,[42,51] and amide carbon (NH—C═O) bond in chitosan backbone[42] at the binding energies of ∼285, ∼ 286.5, and ∼288 eV, respectively. Figure 1B,C illustrated the C_{1s} spectrum of ACA and $ACAC_{PEG}$ membranes. Except for the three peaks above, there appeared to be one more peak at a binding energy of ∼289 eV due to the carboxyl carbon (O═C—O^-) in alginate.[51,53] Figure 1D,E,F showed the O_{1s} spectrum of CS-g-MPEG2K-DS21%, ACA, and $ACAC_{PEG}$ membranes, respectively. Peaks at ∼530, ∼ 531, and ∼533 eV arose from the O═C—O^- group in alginate,[53] the HN—C═O of chitosan backbone,[42] and the C−O−C of MPEG side chains,[42] respectively.

For XPS measurement, the peak height or area of C−O−C peak was influenced by several factors including the photoelectron productivity (γ) and nonlinear mean free path (λ), which both had relationship with material properties.[54] Therefore, the relative intensity of C−O−C peak to O═C—O^-, O═C—NH, and C−C peaks rather than C−O−C peak height was assessed to eliminate the influence of the own properties of different materials.[41,50] The relative intensity of peaks at ∼286.5 eV in C_{1s} and ∼533 eV in O_{1s} of $ACAC_{PEG}$ became significantly stronger compared to ACA membranes. A relative increase in C−O−C (∼ 286.5 eV) peak and a relative decrease in C−C (∼ 285 eV) peak were observed, indicating the introduction of MPEG chains on the surface of ACA microcapsules.

To quantitatively describe the MPEG modification on microcapsules, the subsequent peak area percentages of above peaks were calculated according to eq 2. It could be seen in Table 1 that the C−O−C binding state of CS-g-MPEG2K-DS21% dominated in both C_{1s} and O_{1s} peaks, showing the peak area percentages of 78% and 92.9%, respectively, while in ACA membranes, no significant binding state existed. Comparing $ACAC_{PEG}$ with ACA, the peak area percentage of C−O−C in C_{1s} increased from 34.5% to 44.9%, within the range between the ACA control (34.5%) and the CS-g-MPEG copolymer (78%). The percentage in O_{1s} had the same trend. This phenomenon verified the surface modification by MPEG on the microcapsule membrane.

Therefore, C−O−C binding state in high-resolution XPS spectra could be used to analyze the surface of MPEG-modified membranes, verify the attachment of MPEG chains on the membrane, and quantitatively compare the MPEG surface coverage under different grafting parameters including the buffer layer substrate, membrane thickness, and grafting method.

3.3. Effect of Alginate Buffer Layer. The alginate buffer layer will influence the grafting of MPEG chains. Here, the effect of AC and ACA core substrate on n_S of the subsequent grafting of C_{PEG} was studied.

The high-resolution spectra of C_{1s} and O_{1s} peaks of ACC_{PEG} (see Figure S1 of the Supporting Information) and $ACAC_{PEG}$ (Figure 1) membranes and their fitting curves were compared. The relative intensity of C−O−C peaks at ∼286.5 and ∼533 eV of $ACAC_{PEG}$ were both stronger than that of ACC_{PEG}. The peak area percentage of C−O−C in C_{1s} of $ACAC_{PEG}$ (44.9%, see Table 1) was higher than that of ACC_{PEG} (37.0%, see Table S1 of the Supporting Information), and so was the percentage in O_{1s}, 26.6% for $ACAC_{PEG}$, and 9.9% for ACC_{PEG}. This indicated there were more MPEG chains on the surface of $ACAC_{PEG}$ than that of ACC_{PEG}. The only difference can be attributed to the alginate buffer layer in $ACAC_{PEG}$ compared to ACC_{PEG} microcapsule. The AC membrane showed negative charge[47] due to more alginate with negative charge existing on the surface than chitosan with positive charge. The alginate buffer layer was introduced to neutralize the positive charge of chitosan layer in AC membrane, and formed an ACA membrane showing more negative charge than AC. The C_{PEG} also carried positive charge. Therefore, the ACA membrane could graft more C_{PEG} compared to AC membrane through electrostatic interaction.

To provide insight into the alginate buffer layer, the values of n_S calculated by eqs 1−4 in Section 2.5 were listed in Table 2, and the binding amount (m_b, μg/cm^2) of CS-g-MPEG was also calculated by eq 6 in Section 2.6. The m_b showed the total C_{PEG} both on the surface and in the 3D hydrogel network structure, while n_S only reflected the surface information. The m_b on ACC_{PEG} (71 ± 7 μg/cm^2) was remarkably higher than m_b on $ACAC_{PEG}$ microcapsules (36 ± 2 μg/cm^2). However, the n_S of $ACAC_{PEG}$ (0.29 ± 0.07 chains/nm^2) was twice that of ACC_{PEG} (0.14 ± 0.05 chains/nm^2), as shown in Table 2, which indicated that there was more C_{PEG} diffused into ACC_{PEG} than $ACAC_{PEG}$. The alginate buffer layer in $ACAC_{PEG}$ not only acted as a neutralization layer, providing more −COO^- negative binding sites for C_{PEG}, but also restricted the diffusion of C_{PEG}, enriching the surface graft density due to its more compact structure.

CLSM images can visually verify the diffusion-preventing ability of the alginate buffer layer. Figure 2A,B showed CLSM images of ACC_{PEG} and $ACAC_{PEG}$ microcapsules modified by FITC-labeled CS-g-MPEG, respectively, with their corresponding fluorescent intensity profiles of equatorial sections. In the ACC_{PEG} profile, the fluorescent C_{PEG} distributed not only on the surface, but also in the AC core, in which green fluorescence was shown. While in the $ACAC_{PEG}$ profile, the dark appearance of the microcapsules interior, of which the

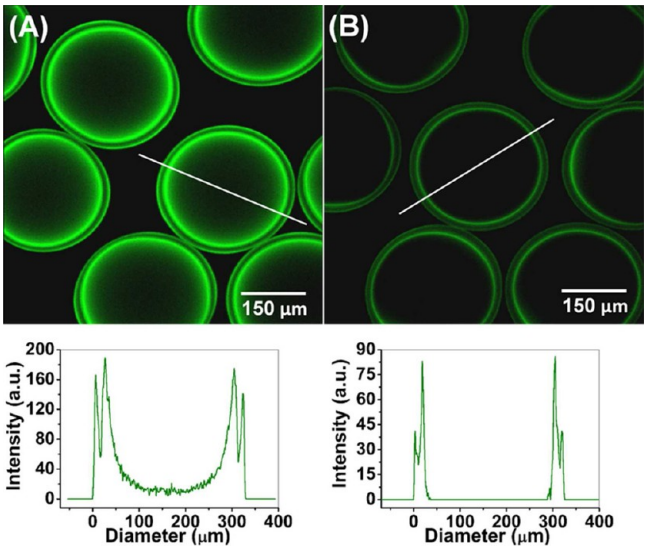

Figure 2. CLSM fluorescent images of microcapsules modified by FITC-labeled CS-g-MPEG2K-DS21% without and with alginate buffer layer: (A) ACC_{PEG} and (B) $ACAC_{PEG}$. The upper and lower micrographs showed the CS-g-MPEG2K-DS21% distributions and their corresponding fluorescent intensity profiles along the white line across the microcapsule diameter, respectively. The micrographs were optical sections taken through the equator of the microcapsules.

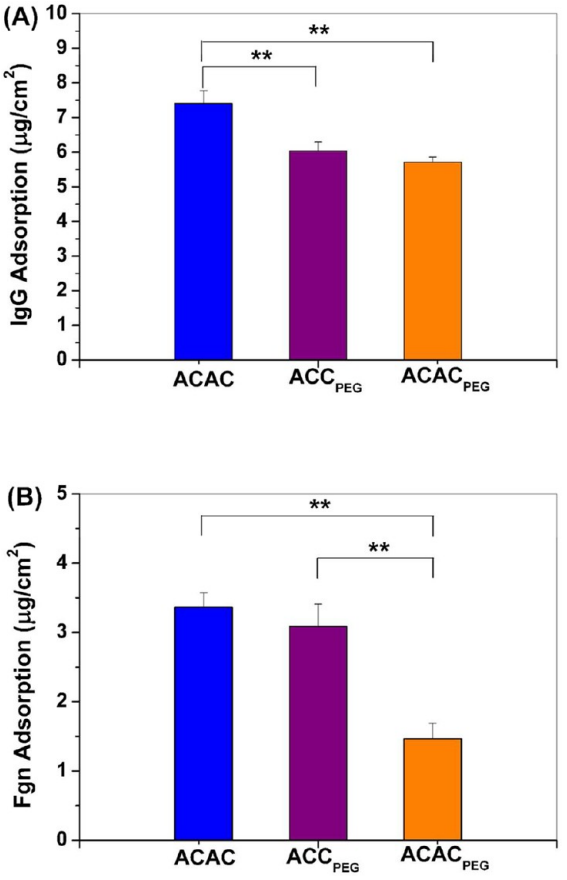

Figure 3. Effect of the alginate buffer layer on IgG (A) and Fgn (B) adsorption on the hydrogel microcapsules modified by CS-g-MPEG2K-DS21% (**$p < 0.01$; $n = 3$).

fluorescence intensity was zero, contrasted with the bright green fluorescence on the surface, demonstrating that the fluorescent C_{PEG} distributed only on the surface and the alginate buffer layer could prevent C_{PEG} from diffusing into the ACA core.

To demonstrate the relationship between n_S and protein repellency, representative proteins IgG and Fgn were chosen as the protein models, because IgG was the main protein that excited immunogenic response against foreign materials[55] and Fgn was the protein that led to fibrosis overgrowth.[56] Based on the method in Section 2.8, the amount of IgG and Fgn adsorption was calculated and shown in Figure 3. The results in Figure 3A demonstrated that the MPEG-modified microcapsules (ACC_{PEG} and $ACAC_{PEG}$) had effective protein repellency compared to ACAC microcapsules with IgG adsorption amount of 7.4 ± 0.4 $\mu g/cm^2$ as control. The MPEG side chains on the surface of microcapsules restricted IgG adsorption due to their steric hindrance, excluded volume, and charge shielding effect compared to the chitosan layer. However, the amount of IgG adsorption on ACC_{PEG} (6.0 ± 0.3 $\mu g/cm^2$) and $ACAC_{PEG}$ (5.7 ± 0.1 $\mu g/cm^2$) microcapsules had no significant difference, although the n_S values of $ACAC_{PEG}$ (0.29 chains/nm^2) were greater than twice that of ACC_{PEG} (0.14 chains/nm^2) microcapsules. This result against law was attributed to the small difference in the number of n_S between them. When d_{abs} was smaller than 3 nm,[43] MPEG chains on both groups mainly existed in a mushroom-like conformation, showing little difference of resistance to protein adsorption between them. This small increase in MPEG surface coverage on $ACAC_{PEG}$ compared to ACC_{PEG} microcapsules was still not enough to effectively restrict proteins from penetrating into the neighboring MPEG chains and adsorbing on the surface. Therefore, the effect of ACC_{PEG} and $ACAC_{PEG}$ on protein repellency demonstrated little difference. However, this could not deny the importance of n_S. When it came to a considerable amount with brush-like structure, n_S would dominate the protein repellency.

Generally, as illustrated in Scheme 2, proteins with pI smaller than 7.4 showed negative charge,[57] which could be adsorbed by AC core more easily than ACA core. IgG protein had a pI[58] of 6.5, which was close to the body environment at pH 7.4. When it came to Fgn with pI[59] of 5.1, the shielding effect of the alginate buffer layer became more obvious. For this reason, $ACAC_{PEG}$ microcapsules (1.5 ± 0.2 $\mu g/cm^2$) showed significant resistant ability against Fgn adsorption compared to ACC_{PEG} (3.1 ± 0.3 $\mu g/cm^2$) and ACAC (3.4 ± 0.2 $\mu g/cm^2$) microcapsules in Figure 3B. The amount of Fgn adsorption on ACC_{PEG} microcapsules was much higher than that on $ACAC_{PEG}$ microcapsules. Moreover, ACC_{PEG} microcapsules showed no significantly different amount of Fgn adsorption compared to ACAC microcapsules. This is because, on the surface with such n_S, there was still a large number of positive places available for Fgn protein adsorption on ACC_{PEG} microcapsules.[60]

Meantime, the surface potentials of ACC_{PEG} and $ACAC_{PEG}$ microcapsules were measured to further verify the interaction between protein and modified surface. The ACC_{PEG} and $ACAC_{PEG}$ microcapsules exhibited zeta potential of −4.6 ± 0.3 and −5.6 ± 0.3 mV at pH 7.4, respectively. The absolute value of zeta potential of ACC_{PEG} was lower than that of $ACAC_{PEG}$ microcapsules, which confirmed that ACC_{PEG} without alginate buffer layer had more positive sites for Fgn adsorption compared to $ACAC_{PEG}$ microcapsules. Therefore, when the

dx.doi.org/10.1021/la302615t | Langmuir 2012, 28, 13261−13273

Scheme 2. Schematic Illustration of the Adsorption Behavior of IgG and Fgn Proteins with Different pI on the ACC_{PEG} and $ACAC_{PEG}$ Microcapsules with the Same MPEG Surface Graft Density (not to scale)

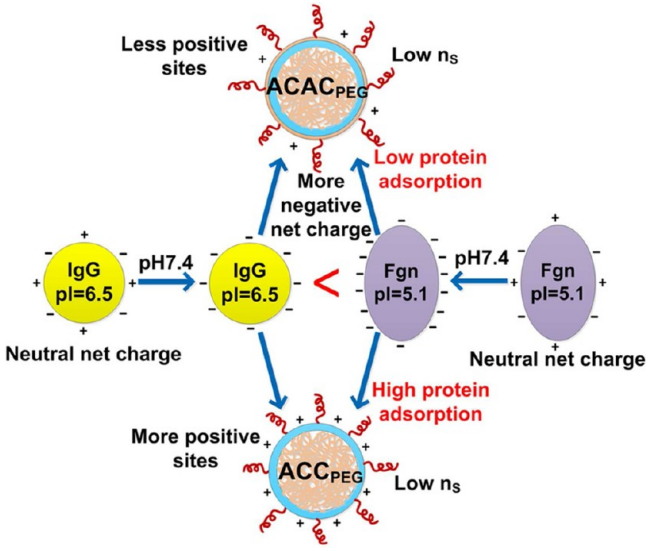

MPEG surface graft density is not high, the electrostatic interaction between protein and microcapsule surfaces would play an important role.

The introduction of alginate buffer layer mainly showed three functions, providing $-COO^-$ negative sites for C_{PEG} binding and preventing the diffusion of C_{PEG} into microcapsules to increase n_S, and neutralizing the charge to avoid protein adsorption, which had been verified by the adsorption of IgG and Fgn. The overall protein repellency of $ACAC_{PEG}$ was better than ACC_{PEG}. The n_S and surface charge both had influence on protein adsorption.[60] Therefore, $ACAC_{PEG}$ microcapsules modified by MPEG with alginate buffer layer were chosen to study the influence of membrane thickness on n_S and protein repellency below.

3.4. Effect of Membrane Thickness. In $ACAC_{PEG}$ microcapsules, the membrane thickness was defined as the depth of AC mixed layer, formed by the diffusion of chitosan into calcium alginate gels. As coating time increased, the membrane thickness increased because more chitosan diffused into and bound onto gels. Therefore, more alginate with negative charge was subsequently used for neutralizing to provide more $-COO^-$ negative binding sites on the surface of ACA microcapsules, which were favorable for C_{PEG} grafting. To sum up, the thicker the membrane was, the more alginate for neutralization and the higher the n_S was.

To confirm the former inference, ACA microcapsules treated with rhodamine B-labeled chitosan and fluoresceinamine-labeled alginate were prepared and examined by CLSM. The images were taken and thereafter quantified by computational analysis described in Section 2.7. Figure 4 showed CLSM images and the corresponding fluorescence intensity profiles of the microcapsules with different membrane thicknesses. The green and red fluorescence represented alginate and chitosan, respectively. The intensity and width of the red fluorescence signal increased with the membrane thickness, indicating the increasing of chitosan coated on gels. The same trend was also observed in green fluorescence signal representing alginate. For 10 μm sample (Figure 4A), green fluorescence could be hardly

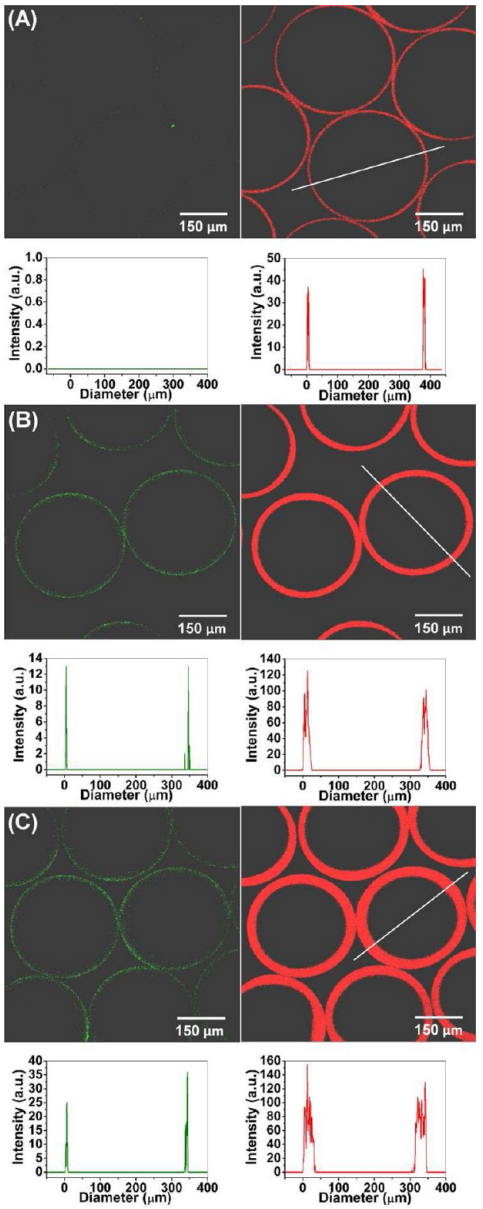

Figure 4. CLSM images of fluorescent-labeled ACA microcapsules with different membrane thicknesses of (A) 10, (B) 20, and (C) 40 μm. The left and right micrographs (upper) showed the alginate buffer layer (green) and chitosan (red) distributions and their corresponding fluorescent intensity profiles (lower) along the white line across the microcapsule diameter, respectively. The micrographs were optical sections taken through the equator of the microcapsules.

detected by CLSM. For 20 (Figure 4B) and 40 μm (Figure 4C) samples, the signal was strengthened, which meant more alginate coated on ACA membranes. Besides qualitative and visual analysis of the images, we developed a quantitative analysis method, which could effectively value the material fluorescent intensity and reflect the inherent law. For better understanding, the fluorescent intensity was integrated along the diameter and summarized in Table 3. The concentration of alginate on the 40 μm sample (544 ± 85) was more than twice that on the 20 μm sample (235 ± 80). The fluorescence of alginate on the 10 μm sample was almost undetectable by CLSM. Therefore, the amount of coating alginate increased with increasing membrane thickness.

dx.doi.org/10.1021/la302615t | *Langmuir* 2012, 28, 13261−13273

Table 3. Fluorescent Intensity of Chitosan and Alginate Buffer Layer on the ACA Hydrogel Microcapsules with Different Membrane Thicknesses

	fluorescent intensity[a]	
membrane thickness (μm)	chitosan (red)	alginate (green)
10	2358 ± 804	0
20	8549 ± 1237	235 ± 80
40	17257 ± 1516	544 ± 85

[a]Expressed as mean ± SD (n = 12).

The C_{1s} and O_{1s} species scans at ~286.5 and ~533 eV showed the growing relative intensity of the C−O−C peak as the membrane thickness increased (see Figure S2 of the Supporting Information). As the membrane thickness increased from 10 to 40 μm, the C−O−C peak area percentage in C_{1s} increased from 38.6% to 78.0% and that in O_{1s} also increased from 10.5% to 34.0% (see Table S2 of the Supporting Information), which qualitatively demonstrated the increase in n_S. To quantify, n_S increased significantly from 0.06 ± 0.04 to 0.74 ± 0.03 chains/nm^2 with membrane thickness from 10 to 40 μm (shown in Table 2), which confirmed the conclusion drawn by the increase in relative intensity of the C−O−C peaks in C_{1s} and O_{1s}.

The influence of the membrane thickness on protein adsorption was also investigated. The IgG adsorption results (Figure 5A) showed that q decreased from 9.1 ± 0.3 to 4.5 ± 0.2 μg/cm^2, exhibiting a reduction of ~50%, as the membrane thickness increased from 10 to 40 μm. The Fgn adsorption (Figure 5B) also decreased from 4.1 ± 0.2 to 1.6 ± 0.2 μg/cm^2, showing a reduction of ~61%. The main reason for better protein repellency was that the n_S increased ten times for 40 μm sample compared to 10 μm sample. When n_S was small, the protein repellency was not significant as described in Section 3.3. However, when it reached a considerable amount (0.74 ± 0.03 chains/nm^2), the n_S played an important role in resisting proteins. In this case, the space between neighboring MPEG chains became narrower as the increase in n_S and the proteins were more hindered to reach surface sites on $ACAC_{PEG}$ microcapsules so that there was a decrease in adsorption for both IgG and Fgn proteins.

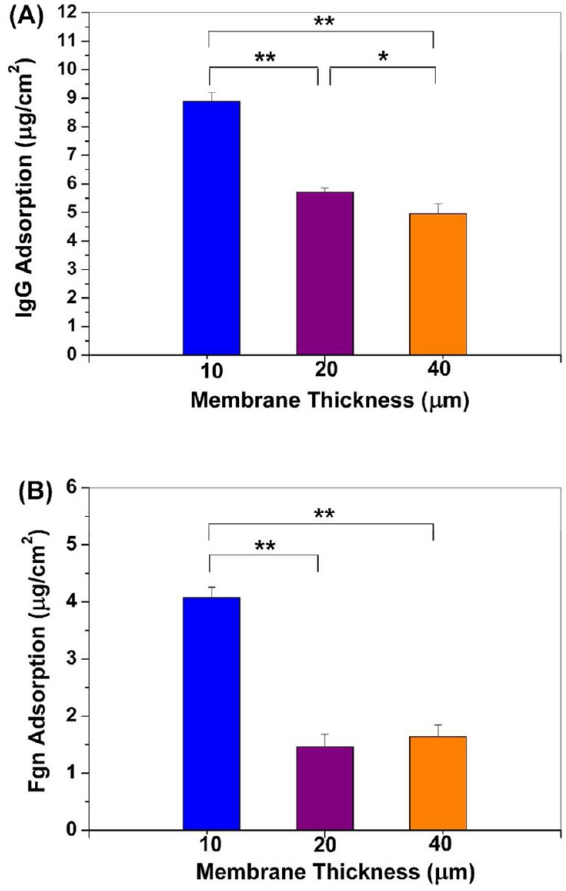

Figure 5. Effect of the membrane thickness on IgG (A) and Fgn (B) adsorption on the hydrogel microcapsules modified by CS-g-MPEG2K-DS21% (*p < 0.05, **p < 0.01; n = 3).

Meanwhile, as the membrane thickness increased from 10 to 40 μm, the surface roughness significantly increased from 99 ± 29 to 245 ± 101 nm, as shown in Figure 6. All the three-dimensional morphology of $ACAC_{PEG}$ microcapsules with different membrane thickness appeared to be uniformly structured with almost similar irregularities. Generally, a membrane with greater surface roughness could provide larger surface area for protein adsorption. However, the law of protein adsorption went against the results of surface roughness. This was because the brush-like MPEG chains on the $ACAC_{PEG}$ microcapsules dominated the protein adsorption due to their excluded volume, steric stabilization, and charge shielding effect rather than the surface roughness of microcapsules.

Besides n_S, the surface charge site was another factor that influenced the protein repellency. For IgG, the decrease in protein adsorption and the increase in n_S matched perfectly, which indicated that n_S rather than surface charge dominated in protein repellency. For Fgn, the protein adsorption of 20 and 40 μm samples showed little difference even though the n_S increased from 0.29 ± 0.07 to 0.74 ± 0.03 chains/nm^2. The combination of n_S and surface charge site together affected the Fgn adsorption. The 10 μm sample showed hardly any C_{PEG} grafting chains and the small amount of alginate could not shield the surface positive charge sites, leading to high protein adsorption. When the membrane thickness reached 20 μm, the increase in n_S and the higher amount of alginate, which could shield the charge sites, both promoted protein repellency. As the membrane thickness continually increased to 40 μm, the surface charge effect originating from the large increase in chitosan with positive charge sites dominated the Fgn adsorption.[59] Therefore, the protein repellency showed no more improvement. Anyway, the overall protein repellency improved with the increase in membrane thickness for IgG and Fgn.

3.5. Effect of Grafting Method. The investigations above were all based on MPEG-modified microcapsules by the LBL polyelectrolyte self-assembly method through electrostatic interaction between C_{PEG} and alginate. However, the maximum n_S could only reach 0.74 ± 0.03 chains/nm^2 due to the large steric hindrance of branched structure of CS-g-MPEG copolymer. The brush-like MPEG side chains that had been fixed on microcapsules would restrict the further binding of CS-g-MPEG. Moreover, the decrease in $-COO^-$ negative binding sites was also unfavorable for the copolymer binding process, resulting in the limitation of n_S even optimizing the binding parameters. Therefore, to further improve n_S, changing the grafting method was prospective. For this aim, the in situ covalent grafting method was chosen as an alternative way for enhancing n_S and protein repellency. The in situ covalent

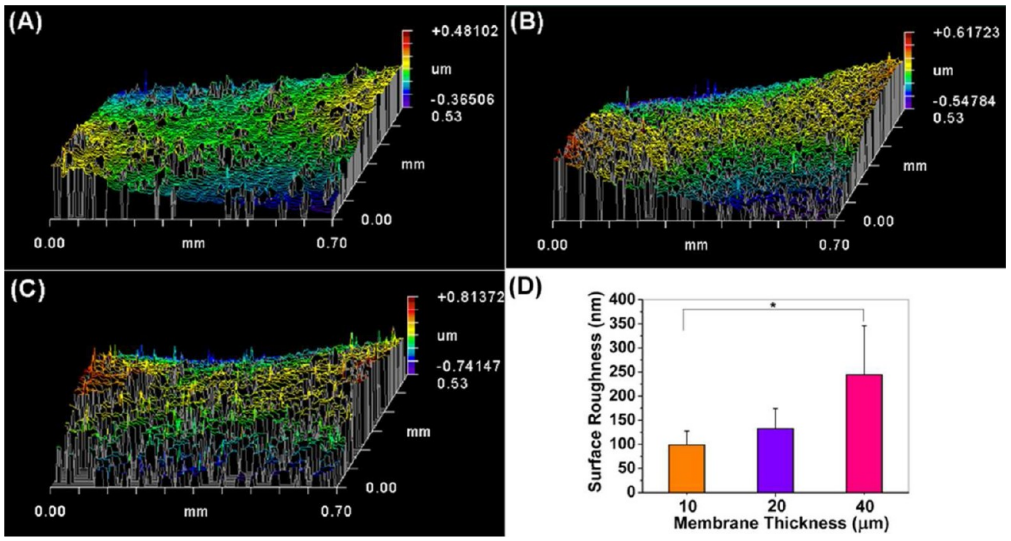

Figure 6. Three-dimensional surface morphology of $ACAC_{PEG}$ microcapsules with membrane thickness of (A) 10, (B) 20, and (C) 40 μm, respectively, and the surface roughness (D) of $ACAC_{PEG}$ microcapsules with different membrane thickness ($^*p < 0.05$; $n = 3$).

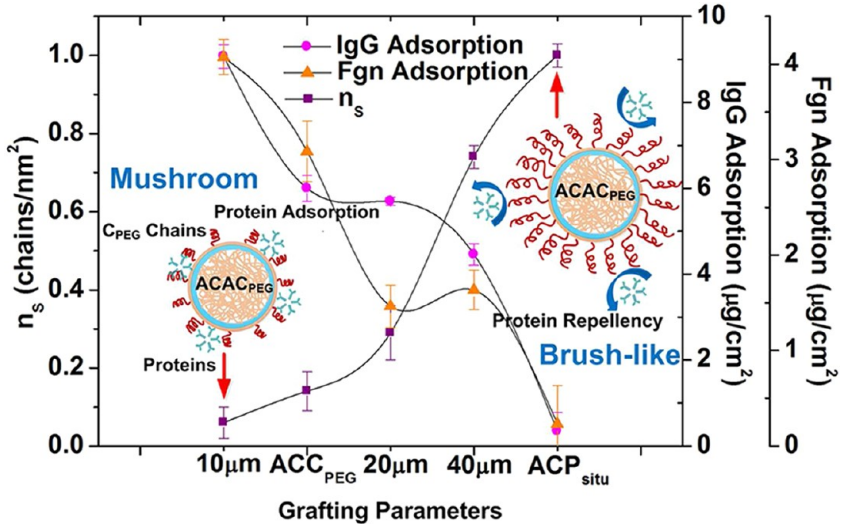

Figure 7. Variation of n_S, IgG adsorption, and Fgn adsorption corresponding to different grafting parameters. Insets: the schematic illustration of the mushroom conformation (left) and the brush-like conformation (right) of MPEG chains (not to scale).

grafting in this work was defined as a method that the modification reaction happened directly on the fabricated microcapsules through covalent link by the product of in situ hydrolysis of MPEG-BADA without purification or prior synthesis of MPEG-grafted copolymer.

The modification process was mentioned in Section 2.2.2. It was generally considered that the terminal aldehyde MPEG (MPEG-CHO) chains could freely diffuse into the 3D hydrogel network structure of membrane and bind onto the $-NH_2$ groups of chitosan in the AC core through Schiff-base reaction. MPEG chains could be fixed onto microcapsules by covalent link with long-term stability. Moreover, the compact MPEG chains modification could also be obtained because of their smaller steric hindrance. XPS results (see Figure S3 of the Supporting Information) showed that the relative intensity of C−O−C peaks in C_{1s} and O_{1s} of ACP_{situ} membranes enhanced remarkably compared to that of AC membranes (see Figure S1 of the Supporting Information), indicating the introduction of MPEG chains. According to the increase in peak area percentage of C−O−C in C_{1s} from 31.2% to 69.5%, n_S was calculated as 1.00 ± 0.03 chains/nm^2 by eq 5. At this surface graft density of MPEG, IgG and Fgn protein adsorption prominently decreased to 0.3 ± 0.4 and 0.2 ± 0.4 μg/cm^2, respectively, both showing a reduction of ∼100% compared to the ACAC control (Figure 7). This microcapsule surface modified by MPEG through in situ covalent grafting method was almost immune to protein adsorption. In this case, IgG and Fgn proteins had the same adsorption tendency in spite of their differing amounts of negative charge ionized at pH 7.4. This was because the MPEG single chain could insert into the AC microcapsule membrane with smaller steric hindrance resulting in compact accumulation of MPEG chains. Moreover, the MPEG chains on the surface were close enough to shield the surface charge so that the surface graft density effect dominated protein adsorption behavior rather than surface charge effect.[59]

MPEG-modified hydrogel microcapsules had prominent protein repellency. Moreover, by adjusting the grafting parameters, both IgG and Fgn adsorption decreased sharply

dx.doi.org/10.1021/la302615t | Langmuir 2012, 28, 13261−13273

with increase in n_S, as shown in Figure 7. When n_S was less than ~0.3 chains/nm^2, the space distance of neighboring MPEG chains was too large, making MPEG chains distribute separately and collapse as mushroom conformation on the surface with little protein repellency. As n_S increased to more than ~0.7 chains/nm^2, the conformation of MPEG chains exhibited the combination of mushroom and brush-like which had better repellency against IgG and Fgn adsorption. When n_S increased to 1.00 ± 0.03 chains/nm^2, the space distance of neighboring MPEG chains decreased sharply, and thus, MPEG chains stretched out away from microcapsule surface to form brush-like conformation through interchain steric repulsion.[61] The brush-like MPEG chains had the best protein repellency due to their excluded volume, steric stabilization, and charge shielding effect. Therefore, neutralization with alginate, increase in the membrane thickness, and in situ covalent grafting method were all effective ways to concentrate MPEG chains on the surface of microcapsules and improve protein repellency of microcapsules modified by MPEG.

4. CONCLUSIONS

Enhancement of surface graft density of MPEG on alginate/chitosan hydrogel microcapsules for better protein repellency was achieved by controlling the buffer layer substrate, membrane thickness, and grafting method. The alginate buffer layer and increase in membrane thickness were proposed to hinder the diffusion of MPEG chains and provide more $-COO^-$ negative binding sites. The in situ covalent grafting method was also established to liberate MPEG side chains from chitosan backbone without steric hindrance. Moreover, the XPS model was developed to quantitatively study the relationship between n_S and protein repellency.

The results indicated that $ACAC_{PEG}$ with alginate buffer layer had higher n_S of MPEG chains on the outermost portion of microcapsule membrane, and showed more promise than ACC_{PEG} in protein repellency. The n_S values increased with the amount of alginate buffer layer, when the membrane thickness of $ACAC_{PEG}$ microcapsules increased from 10 to 40 μm. MPEG surface modification by the in situ covalent grafting method attained n_S of 1.00 ± 0.03 chains/nm^2, which was almost completely immune to protein adsorption. As n_S became high enough, the excluded volume, steric stabilization, and charge shielding effect of stretching MPEG chains dominated, exhibiting the best protein repellency.

This work laid a solid foundation for surface modification and quantitative analysis of the interaction between biomacromolecules and hydrogel with a 3D network structure. This antifouling hydrogel biomaterial may have great potential for transplantation in vivo.

■ ASSOCIATED CONTENT

Supporting Information

High resolution XPS spectra for dehydrated AC and ACC_{PEG} microcapsule membranes, $ACAC_{PEG}$ microcapsule membranes with different membrane thicknesses, and ACP_{situ} microcapsule membranes, and their fitting curves; the peak area percentage and binding energy data for carbon and oxygen species of the MPEG-modified microcapsules with different grafting parameters in a high resolution mode measured by XPS. This material is available free of charge via the Internet at http://pubs.acs.org.

■ AUTHOR INFORMATION

Corresponding Author

*E-mail: liuxd@dicp.ac.cn (Xiudong Liu); xiehg@dicp.ac.cn (Hongguo Xie). Tel: 86-411-84379139. Fax: 86-411-84379096.

Notes

The authors declare no competing financial interest.

■ ACKNOWLEDGMENTS

This project was supported by the National Basic Research Program of China (grant 2012CB720801), the National Natural Science Foundation of China (grant 10979050, 51103157), "Strategic Priority Research Program" of the Chinese Academy of Sciences, Stem Cell and Regenerative Medicine Research (grant XDA01030303), and the National Key Sci-Tech Special Project of China (grant 2012ZX10002011-013).

■ REFERENCES

(1) Chang, T. M. Semipermeable microcapsules. *Science* **1964**, *146*, 524−525.
(2) Lim, F.; Sun, A. M. Microencapsulated islets as bioartificial endocrine pancreas. *Science* **1980**, *210*, 908−910.
(3) Chang, T. M. S. Artificial cells for cell and organ replacements. *Artif. Organs* **2004**, *28*, 265−270.
(4) Orive, G.; Gascon, A. R.; Hernandez, R. M.; Igartua, M.; Pedraz, J. L. Cell microencapsulation technology for biomedical purposes: novel insights and challenges. *Trends. Pharmacol. Sci.* **2003**, *24*, 207−210.
(5) Elisseeff, J. Hydrogels: Structure starts to gel. *Nature* **2008**, *7*, 271−273.
(6) Polizzotti, B. D.; Fairbanks, B. D.; Anseth, K. S. Three-Dimensional Biochemical Patterning of Click-Based Composite Hydrogels via Thiolene Photopolymerization. *Biomacromolecules* **2008**, *9*, 1084−1087.
(7) Benoit, D. S. W.; Schwartz, M. P.; Durney, A. R.; Anseth, K. S. Small functional groups for controlled differentiation of hydrogel-encapsulated human mesenchymal stem cells. *Nat. Mater.* **2008**, *7*, 816−823.
(8) Zielinski, B. A.; Aebischer, P. Chitosan as a matrix for mammalian cell encapsulation. *Biomaterials* **1994**, *15*, 1049−1056.
(9) Chandy, T.; Mooradian, D. L.; Rao, G. H. R. Evaluation of modified alginate-chitosan-polyethylene glycol microcapsules for cell encapsulation. *Artif. Organs* **1999**, *23*, 894−903.
(10) Limor, B.; Marcelle, M. Alginate-chitosan complex coacervation for cell encapsulation: Effect on mechanical properties and on long-term viability. *Biopolymers* **2006**, *82*, 570−579.
(11) Tasima, H.; Hongmei, C.; Wei, O.; Christopher, M.; Bisi, L.; Aleksandra, M. U.; Satya, P. In vitro study of alginate−chitosan microcapsules: an alternative to liver cell transplants for the treatment of liver failure. *Biotechnol. Lett.* **2005**, *27*, 317−322.
(12) Zhang, W. J.; Li, B. G.; Zhang, C.; Xie, X. H.; Tang, T. T. Biocompatibility and membrane strength of C3H10T1/2 cell-loaded alginate-based microcapsules. *Cytotherapy* **2008**, *10*, 90−97.
(13) Blanka, R. Immunocompatibility and biocompatibility of cell delivery systems. *Adv. Drug Delivery Rev.* **2000**, *42*, 65−80.
(14) Lee, J. H.; Lee, H. B.; Andrades, J. D. Blood compatibility of poly (ethylene oxide) surfaces. *Prog. Polym. Sci.* **1995**, *20*, 1043−1079.
(15) Harris, J. M. *Poly(ethylene glycol) Chemistry: Biotechnical and Biomedical Applications*; Plenum Press: New York, 1992; Chapter 1.
(16) Zhou, Y.; Liedberg, B.; Gorochovceva, N.; Makuska, R.; Dedinaite, A.; Claesson, P. M. Chitosan-N-poly (ethylene oxide) brush polymers for reduced nonspecific protein adsorption. *J. Colloid Interface Sci.* **2007**, *305*, 62−71.
(17) Stephanie, P.; Susan, M.; De, P.; Janos, V.; Nicholas, D.; Textor, M. Poly (l-lysine)-graft-poly (ethylene glycol) Assembled Monolayers on Niobium Oxide Surfaces: A Quantitative Study of the Influence of

Polymer Interfacial Architecture on Resistance to Protein Adsorption by ToF-SIMS and in Situ OWLS. *Langmuir* **2003**, *19*, 9216−9225.
(18) Gregory, L.; Kenausis, J. V.; Donald, L. E.; Huang, N. P.; Rolf, H.; Laurence, R. T.; Textor, M.; Jeffrey, A. H.; Nicholas, D. S. Poly (L-lysine)-g-Poly (ethylene glycol) Layers on Metal Oxide Surfaces: Attachment Mechanism and Effects of Polymer Architecture on Resistance to Protein Adsorption. *J. Phys. Chem.* **2000**, *B104*, 3298−3309.
(19) Huang, N. P.; Roger, M.; Janos, V.; Textor, M.; Rolf, H.; Antonella, R.; Donald, L. E.; Jeffrey, A. H.; Nicholas, D. S. Poly (l-lysine)-g-poly (ethylene glycol) Layers on Metal Oxide Surfaces: Surface-Analytical Characterization and Resistance to Serum and Fibrinogen Adsorption. *Langmuir* **2001**, *17*, 489−498.
(20) Gorochovceva, N.; Naderi, A.; Dedinaite, A.; Makuska, R. Chitosan-N-poly (ethylene glycol) brush copolymers: Synthesis and adsorption on silica surface. *Eur. Polym. J.* **2005**, *41*, 2653−2662.
(21) Rundqvist, J.; Hoh, J. H.; Haviland, D. B. Poly (ethylene glycol) Self-Assembled Monolayer Island Growth. *Langmuir* **2005**, *21*, 2981−2987.
(22) Geoffrey, O.; Joseph, I.; Evgeni, P.; Ricardas, M.; Ausvydas, V.; Claesson, P. M. Adsorption Characteristics of Bottle-Brush Polymers on Silica: Effect of Side Chain and Charge Density. *Langmuir* **2008**, *24*, 5341−5349.
(23) Huang, N. P.; De Paul, S. M.; Textor, M. Docking Sites": Nanometer-Scale Organization of a Reactive, Protein-resistant, Graft Copolymer-Based Interface for Macromolecule Immobilization. *Biomacromolecules* **2011**, *12*, 4213−4220.
(24) Alexander, S. Polymer adsorption on small spheres. A scaling approach. *J. Phys. (Paris)* **1977**, *38*, 977−981.
(25) de Gennes, P. G. Polymers at an interface; a simplified view. *Adv. Colloid Interface Sci.* **1987**, *27*, 189−209.
(26) Zheng, J. N.; Xie, H. G.; Yu, W. T.; Liu, X. D.; Xie, W. Y.; Zhu, J.; Ma, X. J. Chitosan-g-MPEG-Modified Alginate/Chitosan Hydrogel Microcapsules: A Quantitative Study of the Effect of Polymer Architecture on the Resistance to Protein Adsorption. *Langmuir* **2010**, *26*, 17156−17164.
(27) Terbojevich, M.; Cosani, A.; Focher, B.; Marsano, E. High-performance gel-permeation chromatography of chitosan samples. *Carbohydr. Res.* **1993**, *250*, 301−314.
(28) Zhao, Y. J.; Zhai, Y. Q.; Ma, G. H.; Su, Zh. G. Kinetic analysis and improvement of the Williamson reaction for the synthesis of poly (ethylene glycol) propionaldehyde. *J. Appl. Polym. Sci.* **2009**, *111*, 1638−1643.
(29) Strand, B. L.; Morch, Y. A.; Espevik, T.; Skjak-Braek, G. Visualization of alginate−poly-L-lysine−alginate microcapsules by confocal laser scanning microscopy. *Biotechnol. Bioeng.* **2003**, *82*, 386−394.
(30) Yu, W. T.; Song, H. Y.; Zheng, G. SH.; Liu, X. D.; Zhang, Y.; Ma, X. J. Study on membrane characteristics of alginate-chitosan microcapsule with cell growth. *J. Membr. Sci.* **2011**, *377*, 214−220.
(31) Onishi, H.; Machida, Y. Biodegradation and distribution of water-soluble chitosan in mice. *Biomaterials* **1999**, *20*, 175−182.
(32) Ohno, K.; Akashi, T.; Tsujii, Y.; Yamamoto, M.; Tabata, Y. Blood Clearance and Biodistribution of Polymer Brush-Afforded Silica Particles Prepared by Surface-Initiated Living Radical Polymerization. *Biomacromolecules* **2012**, *13*, 927−936.
(33) Cvitas, J. T.; Hasan, E.; Ramstedt, M.; Li, X.; Cooper, M.; Abell, C.; Huck, W. T. S.; Gautrot, J. E. Biofunctionalized Protein Resistant Oligo (ethylene glycol)-Derived Polymer Brushes as Selective Immobilization and Sensing Platforms. *Bimacromolecules* **2009**, *10*, 2885−2894.
(34) Tria, M. C. R.; Grande, C. D. T.; Ponnapati, R. R.; Advincula, R. C. Electrochemical Deposition and Surface-Initiated RAFT Polymerization: Protein and Cell-Resistant PPEGMEMA Polymer Brushes. *Biomacromolecules* **2010**, *11*, 3422−3431.
(35) Wattendorf, U.; Kreft, O.; Textor, M.; Sukhorukov, G. B.; Merkle, H. P. Stable Stealth Function for Hollow Polyelectrolyte Microcapsules through a Poly (ethylene glycol) Grafted Polyelectrolyte Adlayer. *Biomacromolecules* **2008**, *9*, 100−108.
(36) Gon, S.; Bendersky, M.; Ross, J. L.; Santore, M. M. Manipulating Protein Adsorption using a Patchy Protein-Resistant Brush. *Langmuir* **2010**, *26*, 12147−12154.
(37) Susan, J.; Sofia, V.; Premnath; Edward, W. M. Poly (ethylene oxide) Grafted to Silicon Surfaces: Grafting Density and Protein Adsorption. *Macromolecules* **1998**, *31*, 5059−5070.
(38) Bentley, M. D.; Roberts, M. J.; Harris, J. M. Reductive amination using poly (ethylene glycol) acetaldehyde hydrate generated in situ: Applications to chitosan and lysozyme. *J. Pharm. Sci.* **1998**, *87*, 1446−1449.
(39) Babensee, J. E.; Sodhi, R. N. S.; Sefton, M. V. X-Ray photoelectron spectroscopy (XPS) surface analysis of HEMA-MMA microcapsules. *J. Biomater. Sci. Polym. Ed.* **1997**, *8*, 655−665.
(40) Xie, H. G.; Li, X. X.; Lv, G. J.; Xie, W. Y.; Zhu, J.; Thomas, L.; Ma, R.; Ma, X. J. Effect of surface wettability and charge on protein adsorption onto implantable alginate-chitosan-alginate microcapsule surfaces. *J. Biomed. Mater. Res.* **2010**, *A92*, 1357−1365.
(41) Zahr, A. S.; de Villiers, M.; Pishko, M. V. Encapsulation of Drug Nanoparticles in Self-Assembled Macromolecular Nanoshells. *Langmuir* **2005**, *21*, 403−410.
(42) Ruiz-Taylor, L. A.; Martin, T. L.; Wagner, P. X-ray Photoelectron Spectroscopy and Radiometry Studies of Biotin-Derivatized Poly (l-lysine)-grafted-Poly (ethylene glycol) Monolayers on Metal Oxides. *Langmuir* **2001**, *17*, 7313−7322.
(43) Damodaran, V. B.; Fee, C. J.; Ruckh, T.; Popat, K. C. Conformational Studies of Covalently Grafted Poly (ethylene glycol) on Modified Solid Matrices Using X-ray Photoelectron Spectroscopy. *Langmuir* **2010**, *26*, 7299−7306.
(44) Tao, S. L.; Popat, K. C.; Norman, J. J.; Desai, T. A. Surface Modification of SU-8 for Enhanced Biofunctionality and Nonfouling Properties. *Langmuir* **2008**, *24*, 2631−2636.
(45) Yu, W. T.; Lin, J. Z.; Liu, X. D.; Xie, H. G.; Zhao, W.; Ma, X. J. Quantitative characterization of membrane formation process of alginate-chitosan microcapsules by GPC. *J. Membr. Sci.* **2010**, *346*, 296−301.
(46) Ratner, B. D.; Bryant, S. J. Biomaterials: Where We Have Been and Where We Are Going. *Annu. Rev. Biomed. Eng.* **2004**, *6*, 41−75.
(47) Xie, H. G.; Zheng, J. N.; Li, X. X.; Liu, X. D.; Zhu, J.; Wang, F.; Xie, W. Y.; Ma, X. J. Effect of surface morphology and charge on the amount and conformation of fibrinogen adsorbed onto alginate/chitosan microcapsules. *Langmuir* **2010**, *26*, 5587−5594.
(48) Lyons, J. S.; Furlong, D. N.; Homola, A.; Healy, T. W. A Radial Flow Streaming Potential Apparatus for Electrokinetic Studies of Sheet or Plate Materials. *Aust. J. Chem.* **1981**, *34*, 1167−1175.
(49) Werner, C.; Korber, H.; Zimmermann, R.; Dukhin, S.; Jacobasch, H. J. Extended Electrokinetic Characterization of Flat Solid Surfaces. *J. Colloid Interface Sci.* **1998**, *208*, 329−346.
(50) Zahr, A. S.; Davis, C. A.; Pishko, M. V. Macrophage Uptake of Core−Shell Nanoparticles Surface Modified with Poly (ethylene glycol). *Langmuir* **2006**, *22*, 8178−8185.
(51) Fan, X. W.; Lin, L. J.; Messersmith, P. B. Cell fouling resistance of polymer brushes grafted from Ti substrates by surface-initiated polymerization: Effect of ethylene glycol side chain length. *Biomacromolecules* **2006**, *7*, 2443−2448.
(52) Groll, J.; Ademovic, Z.; Ameringer, T.; Klee, D.; Moeller, M. Comparison of Coatings from Reactive Star Shaped PEG-stat-PPG Prepolymers and Grafted Linear PEG for Biological and Medical Applications. *Biomacromolecules* **2005**, *6*, 956−962.
(53) Tama, S. K.; Dusseault, J.; Polizu, S.; Menard, M.; Halle, J. P.; Yahia, L. Physicochemical model of alginate-poly-l-lysine microcapsules defined at the micrometric/nanometric scale using ATR-FTIR, XPS, and ToF-SIMS. *Biomaterials* **2005**, *26*, 6950−6961.
(54) Moudler, J. F.; Stickle, W. F.; Sobol, P. E. Bomben, K. D. *Handbook of X-ray Photoelectron Spectroscopy*; Perkin-Elmer Corporation, 1992.
(55) Bastian, F.; Stelzmuller, M. E.; Kratochwill, K.; Kasimir, M. T.; Simon, P.; Weigel, G. IgG deposition and activation of the classical complement pathway involvement in the activation of human

granulocytes by decellularized porcine heart valve tissue. *Biomaterials* **2008**, *29*, 1824−1832.
(56) Franz, S.; Rammelt, S.; Scharnweber, D.; Simon, J. C. Immune responses to implants-a review of the implications for the design of immunomodulatory biomaterials. *Biomaterials* **2011**, *32*, 6692−6709.
(57) Gon, S.; Fang, B.; Santore, M. M. Interaction of Cationic Proteins and Polypeptides with Biocompatible Cationically-Anchored PEG Brushes. *Macromolecules* **2011**, *44*, 8161−8168.
(58) Cann, J. R.; Brown, R. A.; Kirkwood, J. G. Application of electrophoresis-convection to the fractionation of bovine v-globulin. *J. Biol. Chem.* **1949**, *181*, 161−170.
(59) Bajpai, A. K. Fibrinogen adsorption onto macroporous polymeric surfaces: correlation with biocompatibility aspects. *J. Mater. Sci. Mater. Med.* **2008**, *19*, 343−357.
(60) Gon, S.; Santore, M. M. Single Component and Selective Competitive Protein Adsorption in a Patchy Polymer Brush: Opposition between Steric Repulsions and Electrostatic Attractions. *Langmuir* **2011**, *27*, 1487−1493.
(61) Pop-Georgievski, O.; Popelka, S.; Houska, M.; Chvostova, D.; Proks, V.; Rypacek, F. Poly (ethylene oxide) Layers Grafted to Dopamine-melanin Anchoring Layer: Stability and Resistance to Protein Adsorption. *Biomacromolecules* **2011**, *12*, 3232−3242.